Research Square

Preprints are preliminary reports that have not undergone peer review.
They should not be considered conclusive, used to inform clinical practice,
or referenced by the media as validated information.

Arsenate reduction coupled to anaerobic oxidation of methane by members of the Methanoperedenaceae

Simon McIlroy

simon.mcilroy@qut.edu.au

Queensland University of Technology https://orcid.org/0000-0003-3749-8730

Georgina Joyce

The University of Queensland

Xueqin Zhang

University of Queensland https://orcid.org/0000-0001-9628-6004

Andy Leu

Queensland University of Technology https://orcid.org/0000-0002-9882-9364

Yosephine Gumulya

The University of Queensland

Jianhua Guo

University of Queensland https://orcid.org/0000-0002-4732-9175

Gene Tyson

Queensland University of Technology https://orcid.org/0000-0001-8559-9427

Shihu Hu

The University of Queensland https://orcid.org/0000-0002-1858-8872

Article

Keywords:

Posted Date: March 16th, 2026

DOI: https://doi.org/10.21203/rs.3.rs-9109145/v1

License: This work is licensed under a Creative Commons Attribution 4.0 International License.
Read Full License

Additional Declarations: There is **NO** Competing Interest.

Version of Record: A version of this preprint was published at The ISME Journal on September 26th, 2026. See the published version at https://doi.org/10.1093/ismejo/wrag251.

Arsenate reduction coupled to anaerobic oxidation of methane by members of the *Methanoperedenaceae*

Georgina H. Joyce[a,¥,ϕ], Xueqin Zhang[b,ϕ], Andy O. Leu[a], Yosephine Gumulya[a,€], Jianhua Guo[b], Gene W. Tyson[a], Shihu Hu[b,*], Simon J. McIlroy[a,*]

[a] Centre for Microbiome Research, School of Biomedical Sciences, Queensland University of Technology, Translational Research Institute, Brisbane, Australia

[b] Australian Centre for Water and Environmental Biotechnology, The University of Queensland, Brisbane, Australia

[¥] Present address: School of Chemistry and Molecular Biosciences, The University of Queensland, Brisbane, Australia

[€] Present address: School of Agriculture and Food Sustainability, The University of Queensland, Brisbane, Australia

[ϕ] These authors contributed equally

* Corresponding authors:

Simon J. McIlroy: simon.mcilroy@qut.edu.au

Shihu Hu: s.hu@uq.edu.au

Keywords: Anaerobic oxidation of methane, anaerobic methanotrophic archaea, arsenic, biogeochemical cycles

Abstract

Anaerobic methanotrophic '*Candidatus* Methanoperedenaceae' play a key role mitigating methane emissions from freshwater sediments. Members of the family are metabolically versatile, with species coupling anaerobic oxidation of methane (AOM) to the reduction of nitrate, metal oxides and/or humic compounds. Metagenomic analyses have indicated further uncharacterised metabolic diversity, including the potential for AOM coupled to arsenate reduction (As-AOM). While As-AOM has been confirmed as an important methane sink and contributor to arsenic mobilisation in freshwater reservoirs, the underlying microbiological mechanisms remain to be empirically demonstrated. In this study stoichiometric coupling of dissimilatory arsenate reduction to methane oxidation was demonstrated using enrichment cultures of the uncultured type species '*Ca*. Methanoperedens nitroreducens'. Meta-omics revealed that arsenate oxidoreductases were exclusively encoded by '*Ca.* M. nitroreducens' and upregulated under As-AOM conditions, confirming this species was directly responsible. These findings expand our understanding of '*Ca*. Methanoperedenaceae' physiology and demonstrate microbial mechanisms underpinning arsenic mobilisation in freshwater systems, with important implications for climate and public health.

Introduction

'*Candidatus* Methanoperedenaceae' are globally distributed anaerobic methanotrophic archaea (ANME) that play a critical role in mitigating the atmospheric release of methane in freshwater environments. Unlike marine-associated ANME-lineages, which typically depend on syntrophic partnerships with sulphate-reducing bacteria, '*Ca.* Methanoperedenaceae' are metabolically versatile, having been demonstrated to independently couple anaerobic oxidation of methane (AOM) to the reduction of nitrate and metal oxides [1-5]. Comparative genomic analysis has identified that some members of the family may utilise additional terminal electron acceptors for AOM, including selenate, elemental sulphur and arsenate [6].

Arsenate reduction coupled to AOM (As-AOM) is estimated to account for up to ~50% of the mobilisation of arsenic from wetland soils, making it an important microbial process contributing to freshwater arsenic contamination [7-9]. The detection of '*Ca.* Methanoperedenaceae' in soils where As-AOM occurs has led to their suggested involvement in mediating this biogeological process [9-11]. Several '*Ca*. Methanoperedenaceae' metagenome assembled genomes (MAGs), including that of the type species '*Ca.* Methanoperedens nitroreducens', have been reported to encode putative anaerobic oxidoreductases most homologous to bacterial arsenate reductases (*arr*) and arsenite oxidoreductases (*arx*) [6,12]. However, the role of these putative oxidoreductases for '*Ca*. Methanoperedenaceae' is unclear, particularly as they form a separate phylogenetic clade, which could indicate functional divergence [6,13,14]. Shi and colleagues observed a correlation between the transcription of '*Ca.* Methanoperedenaceae' methyl-coenzyme M reductase (*mcrA*), arsenate reductase (*arrA*), and methane oxidation rates for wetland soils, however the *arrA* transcripts were deemed bacterial and unlinked to the ANME species present, leading the authors to suggest an undefined syntrophic partnership between the ANME and bacterial arsenate reducers [9]. A separate study found a correlation between the expression of total community *arrA* transcripts, including those linked to '*Ca*. Methanoperedenaceae', and '*Ca*. Methanoperedenaceae'-like *mcrA* suggesting the involvement of these archaea in As-AOM in rice paddy sediments [15]. However, *arrA* gene expression was dominated (~95%) by other organisms, making it unclear whether As-AOM by '*Ca*. Methanoperedenaceae' contributed to the biogeochemical transformations observed. Collectively, these studies support the hypothesis that members of '*Ca.* Methanoperedenaceae' play a role in As-AOM in the environment; however, direct evidence and a clear understanding of the underlying microbial mechanisms are still lacking.

In this study, comparative genomics of publicly available '*Ca.* Methanoperedenaceae' MAGs was used to assess the prevalence of arsenate metabolism potential in the family. Batch incubation studies were also performed with an enrichment of the nitrate reducing type species '*Ca.* Methanoperedens nitroreducens', which encodes both a putative arsenate reductase (*arr*) and arsenite oxidoreductase (*arx*) complex. Nitrate was substituted for arsenate as the sole electron acceptor for AOM, and the ability of the enrichment to perform As-AOM was assessed using biochemical, metagenomic and

metatranscriptomic analyses. This work delivers the first experimental demonstration that a microorganism can directly mediate As-AOM and examines the adaptive strategies supporting this metabolism for '*Ca*. Methanoperedenaceae'.

Results and Discussion

Comparative genomics of Arr and Arx across '*Ca.* Methanoperedenaceae'

The prevalence of arsenate reductase (*arr*) and arsenite oxidoreductase (*arx*) gene clusters across the '*Ca*. Methanoperedenaceae' was assessed by screening publicly available MAGs representing the family. High-quality (>70% complete, < 10% contamination) MAGs were screened for ArrA and ArxA based on protein phylogeny to functionally characterised reference sequences. A total of 51 high-quality MAGs representing the family were identified, with 11 of these encoding either *arr* or *arx,* or both (**Fig. 1, S1**). These MAGs, representing arsenate metabolising species, were recovered from diverse and globally distributed environmental sites including a deep underground gold mine site[16], a terrestrial mud volcano[17], various arsenic contaminated sediments[6], and from sediment-seeded methane-fed bioreactors[3,5,18] (**Fig 1, S1**). The distributions of *arr* and *arx* do not align with MAG phylogeny (**Fig. 1**), as noted generally for respiratory oxidoreductases encoded by members of the family[6], consistent with gene retention or loss driven by electron-acceptor availability. Only '*Ca*. M. nitroreducens' and BE2012 encoded both *arr* and *arx*, with the gene clusters arranged in tandem (**Supplementary Fig. 1**)

Blastp analysis indicated that Arr and Arx encoded by '*Ca*. Methanoperedens' are most closely related (up to ~76% AAI) to those found in bacteria rather than related archaeal species, suggesting the genes were inherited horizontally from phylogenetically distant organisms (**S2**). Phylogenetic placement and gene synteny analysis suggest three separate horizontal gene transfer (HGT) events, with Methanoperedens-ArrA forming two separate clades (**Fig. 2, Supplementary Fig. 1**). The closest homolog of Kmv03-ArrA belonged to an uncharacterised MAG of the *Dehalococcoidales* order (76.5% identity, **S2**) and ANME-2ab (*Ca.* 'Methanocomedenaceae', 76.1%, **S2**). The '*Ca*. M. nitroreducens' ArrA was found most homologous to a protein encoded by a separate order within the *Dehalococcoidia* class (63.9% identity, **S2**). For Methanoperedens-Arx, the closest homolog was from an uncharacterised *Bacillota* MAG (56% identity, **S2**).

ArrA and ArxA are reported to have distinct, conserved active site motifs which are involved in substrate binding and are suspected to underpin reaction directionality [14]. We found that the active site motif of '*Ca*. Methanoperedens'-ArrA was consistent with bacterial homologs (RGRY, **Fig. 2**). The predicted active site motif for '*Ca*. Methanoperedens'-ArxA, SGRN(Q/R)G [14], was conserved within the family, but is distinct from the motif conserved in experimentally characterised bacterial homologs, XGRGWG (**Fig. 2**). In addition, it was previously reported by Szyttenholm and colleagues (2020) that Arx distribution amongst bacteria is correlated with the ubiquinone (*ubi*) biosynthetic pathway

meanwhile Arr distribution is correlated with the futalosine/menaquinone (*mqn/men*) biosynthetic pathway, likely due to thermodynamic constraints of these quinone/quinol partners. Given that '*Ca*. Methanoperedenaceae' encode the futalosine pathway [19] and that their Arx active-site motif deviates from characterised bacterial homologues, their Arx may not function as a canonical arsenite oxidoreductase.

The *arx* and *arr* gene clusters in '*Ca*. Methanoperedenaceae' contained all required subunits (*arr/arx*ABCD) for expression of the mature Arr/Arx complex as commonly observed in bacteria **Supplementary Fig. 1**) [12,14]. The gene cluster arrangement and direction of the core *arx* genes were also homologous to those observed in bacterial representatives. '*Ca*. Methanoperedenaceae' core *arr* gene clusters were conserved as *arrABCD*, meanwhile bacterial gene clusters often excluded *arrC* or were arranged as *arrABDC*. Some '*Ca*. Methanoperedenaceae' MAGs were found to encode an archaeal *tatA* directly upstream of the *arrA/arxA*-subunit, which mediates the translocation of fully folded proteins encoding a Tat-signal across the pseudoperiplasmic membrane [20]. These genes may be indicative of an adaptation of the species cell architecture to accommodate horizontally-inherited bacterial gene clusters [21].

'*Ca*. M. nitroreducens' enrichment culture mediates As-AOM

The genome-predicted ability of '*Ca.* M. nitroreducens' to mediate As-AOM was also determined using biomass from a long-term enrichment culture performing nitrate-driven AOM [3] and consistently dominated (~30%) by a strain known to encode *arrAB* and *arxAB* [6]. When the enrichment culture biomass was incubated with methane and arsenate (As(V)), the latter was reduced to arsenite (As(III)) within 72 hours with a nearly complete conversion (**Fig. 3A, Supplementary Fig. 2**). Active AOM was observed with arsenate amendment, as evidenced by the steady increase in concentration of $^{13}CO_2$ produced from $^{13}CH_4$ oxidation (**Fig. 3A**), a trajectory analogous to that of canonical nitrate-driven AOM by '*Ca.* M. nitroreducens' (**Fig. 3B**) The $^{13}CO_2$ accumulation rate linked to AOM was 2.0 ± 0.1 μmol h^{-1} in the arsenate-amended incubation (**Fig. 3C**); about 9 times lower than in the nitrate-amended incubation (18.5 ± 0.5 μmol h^{-1}) (Fig. 3B). Kinetic fitting demonstrated near-identical rates of As(V) reduction (8.1 ± 0.2 μmol h^{-1}) and As(III) production (7.4 ± 0.2 μmol h^{-1}). The close correlation between these rates and that of AOM thereby supports a ~4:1 stoichiometry (**Fig. 3D**), consistent with As-AOM (**Eq. 1**).

$$CH_4 + 4HAsO_4^{2-} \rightarrow CO_2 + 4HAsO_3^{2-} + 2H_2O \quad \Delta G^{\circ\prime} \approx -160\ \text{kJ mol}^{-1} \quad (1)$$

These observations collectively support the coupling of arsenate reduction to AOM by the '*Ca*. M. nitroreducens' enrichment culture.

Structure and metabolic activity of the '*Ca.* M. nitroreducens' enrichment community performing As-AOM

Metagenomic analysis of the bioreactor batches recovered 24 high quality (> 70% complete, <10% contamination) MAGs (**S1**). The final MAG set represented ~87% of the metagenome and ~89% of the total metatranscriptome **(Fig. 4A, Supplementary Table 2**). Both the nitrate and arsenate-fed conditions were dominated by '*Ca.* M. nitroreducens' (MAG-ID: Methanoperedens) in the metagenome (average ~31%) and metatranscriptome (average ~80%). Other abundant organisms included unclassified species of the class *Bacteroidota* (~23% relative abundance; MAG-ID Bacteroidota-1) and the family *Melioribacteraceae* (~15% relative abundance; MAG-ID Melioribacteriaceae-1), although each only made up < 2% of the total transcriptome, indicating a relatively low activity. The second most active population based on the metatranscriptome was annamox bacterium '*Candidatus* Kuenenia stuttgartiensis' (MAG-ID Kuenenia), which accounted for ~6 and ~3% of the total TPM for the arsenate and nitrate-fed batches, respectively.

The bioreactor derived MAGs were functionally annotated to identify microbial populations contributing to As-AOM. '*Ca.* M. nitroreducens' was the only population encoding a methane-oxidation pathway, with the methyl-coenzyme M reductase complex (*mcrAGDBC)* highly transcribed, contributing to ~25% of the nitrate-fed batch metatranscriptome, and ~15% of the arsenate-fed metatranscriptome **(Fig. 4A, S2)**. Reductase complexes involved in arsenic-respiration were investigated by screening the MAGs for molybdoenzyme oxidoreductase A-subunits. '*Ca.* M. nitroreducens' was the only population to encode oxidoreductases homologous to *arrA* and *arxA* **(Supplementary Fig. 3)**. MAGs encoding the aerobic arsenite oxidase complex (Aio) were also not detected in the bioreactor batches. For '*Ca.* M. nitroreducens', 17 of the 38 encoded multiheme type *c* cytochromes (MHCs), typically implicated in adaptive extracellular electron pathways for the organism[1,22], were significantly upregulated (padj < 0.005; log2fold change > 1) under As-AOM conditions. Some of these MHCs might be involved in connecting the oxidoreductase complex to the quinone pool, as was suggested previously suggested for '*Ca*. M. nitroreducens' sp. MPEBLZ for the nitrate reductase NarGH [23]. As-AOM by MHC-mediated extracellular electron transfer to syntrophic partners has been previously hypothesised [9], however the absence of bacterial arsenate reductases in our system does not support this hypothesis here. Further characterisation of the differentially expressed MHCs is required to determine their potential role in As-AOM.

Metabolic response of '*Ca.* M. nitroreducens' to As-AOM conditions

The transcriptional response of '*Ca.* M. nitroreducens' to As-AOM compared to nitrate-AOM was examined in more detail. In total, 1205 genes encoded by '*Ca.* M. nitroreducens' were differentially expressed (padj ≤ 0.05) (**S2**). Under arsenate-fed conditions, genes predicted to be involved in arsenic detoxification, stress-response, and motility were highly upregulated by '*Ca*. M. nitroreducens',

potentially due to the toxicity of the added arsenate and accumulated arsenite (**S2**). The stress responses could be an explanation for the observed decrease in AOM rate during As-amended condition (**Fig. 4**).

Both the putative *arrAB* and *arxAB* genes were significantly upregulated by '*Ca*. M. nitroreducens' in the arsenate-fed batch, whilst their nitrate reductase (*narGHI*) was significantly downregulated (**Fig. 4B, S2**). *ArxAB* was the most significantly differentially expressed oxidoreductase, supporting its importance for '*Ca*. M. nitroreducens' under As-AOM conditions (**Fig. 4B, S2**). While the Arr and Arx complexes were originally thought to catalyse only arsenate reduction [24,25] or arsenite oxidation [12,26,27], respectively, more recent research has shown both can operate bidirectionally [13]. Since both are upregulated for the '*Ca.* M. nitroreducens' population under As-AOM conditions, it is possible that both complexes can mediate arsenate reduction for the species (**Fig. 4B**).

Conclusion

Collectively, the results of this study support the ability of '*Ca.* M. nitroreducens' to independently redirect methane-derived electrons to arsenate via HGT-inherited oxidoreductase complexes. The occurrence of Arr and Arx oxidoreductases encoding '*Ca*. Methanoperedenaceae' from globally distributed sampling sites suggests that arsenate may represent a widespread methane sink. This study importantly provides the first direct evidence for the microbial mechanism responsible for As-AOM, further highlighting the remarkable genetic flexibility of the '*Ca*. Methanoperedenaceae', expanding their known roles in linking methane cycling with diverse geochemical cycles. We extend current understanding of the role of '*Ca*. Methanoperedenaceae' in environmental arsenate cycling and mobilisation, building on evidence that iron-reducing members of the family mediate the release of As(V) bound to iron oxides in sediments via reductive dissolution [7,8]. Microbial processes such as these are collectively the primary cause of arsenic leeching from sediment into natural water reservoirs[28] leading to toxic concentrations[29]. Understanding the natural processes that underpin arsenic poisoning, greenhouse gas release, as well as links between them, is crucial to resolving two significant global health burdens.

Materials and Methods

Comparative genomics of *Ca.* 'Methanoperedens' *arrA* and *arxA*

Detection of ArrA/ArxA in Ca. 'Methanoperedenaceae' genomes

Publicly deposited '*Ca*. Methanoperedenaceae' MAGs were identified on the Genome Taxonomy Database (GTDB) Release 10-RS226 and retrieved from NCBI Genbank to survey the prevalence of arsenate metabolising genes within the family. The '*Ca*. M. nitroreducens' putative *arrA* and *arxA* ORFs were used as blast queries to identify homologous proteins in the additional '*Ca*. Methanoperedenaceae' MAGs. Homologous proteins were determined via blastp with the following parameters: query cover $\geq 65\%$, evalue $\leq 1e^{-10}$, percent identity $\geq 25\%$. The putative reductase subunits

and their homologs were subject to phylogenetic analysis alongside a set of curated molybdopterin oxidoreductase A-subunits subunits previous publications [6,12]. Phylogenetic trees were generated by first aligning protein sequences using Muscle v5 [30] with the -super5 parameter, trimming the alignment via trimAl with the automated1 method, and phylogenetic placement was inferred using IQ-Tree [31] ultrafast bootstrap approximation with 1000 replicates.

To identify closer homologs and potential sources of HGT, the set of '*Ca*. Methanoperedenaceae'-ArrA/ArxA proteins, as identified based on phylogeny to characterised bacteria ArrA/ArxA, were used as diamond blastp queries against all redundant protein coding regions published in GTDB Release 10-RS226, excluding those from '*Ca*. Methanoperedenaceae' genomes (query cover ≥ 65%, evalue ≤ $1e^{-10}$, percent identity ≥ 25%, maximum targets = 15). A preliminary protein tree was generated with hits, and proteins most phylogenetically related to '*Ca*. Methanoperedenaceae' were retained to generate a pruned tree. This pruned tree was visualised on iTOL [32] alongside the untrimmed multiple sequence alignment (MSA) of the active site residues and formatted with Adobe Illustrator.

Comparison of Arr/Arx gene operons

The arrangement of the putative Arr and Arx gene clusters found within '*Ca*. Methanoperedenaceae' genomes was compared to other organisms. To do so, genomes of the ArrA/ArxA-encoding organisms were obtained from Genbank. Genomic regions 5 kb upstream and 5 kb downstream of the *arrA* and *arxA* ORFs were extracted and protein coding regions were predicted with Prodigal via Prokka. To identify highly conserved genomic regions, a pairwise alignment was performed using minimap2 with the following parameters: 'minimap2 -X -p 0.1'. The R-packages gggenomes and ggtree were used to visualise the gene clusters, ordered by ArrA/ArxA phylogeny. Gene annotations were inferred using Prokka annotations, operon structures described in previous studies [12,26,27,33], and protein homology.

'*Ca.* M. nitroreducens' enrichment culture

All batch incubations in this study were seeded from an established enrichment culture of '*Ca*. M. nitroreducens' (~30% of the community) performing nitrate-driven AOM. This system was seeded from the original '*Ca*. M. nitroreducens' enrichment of Haroon and colleagues (2013) and operated under similar conditions for >10 years. Briefly, the parent system was a 2 L parent reactor vessel with 1.5 L of liquid and 0.5 L headspace fed weekly with methane (as a gas mix: 90% CH_4, 5% CO_2 and 5% N_2), nitrate (topped up to 14.2 mmol L^{-1}) and ammonium (topped up to 14.2 mmol L^{-1}).

Batch experimentation

Batch incubations were set up in duplicate under two conditions: supplied either (1) arsenate and methane, or (2) nitrate and methane. Batch inoculum was prepared from a 300 mL aliquot of biomass suspension from the parent bioreactor which was incubated in an anoxic vessel to consume the residual nitrate. Nitrate concentration was monitored with nitrate stripes (Merck) until depletion at ~ 8

days. In an anaerobic chamber, 30 mL of inoculum was dispensed into each 58 mL serum bottles. The As-AOM condition batches were amended with 0.5 mM of arsenate from a stock solution (50 mM $Na_2HAsO_4 \cdot 7H_2O$, Sigma-Aldrich). Simultaneously, the nitrate control treatment was amended with 5 mM of nitrate. All treatments were sealed with butyl rubber stoppers clamped with aluminium caps and then flushed with gas mix (95% Ar and 5% CO_2) for 5 min prior to injection of 10 mL ^{13}C-methane (99% atom ^{13}C, Sigma-Aldrich). All batches were incubated on a magnetic stirrer (100 rpm) at 24 ± 2 ^{o}C and incubated over 72 hours.

Geochemical sampling and measurements

Each batch was periodically sampled using an Ar-flushed 3-mL sterile syringe with 25-gague needle. Half of the cell suspension was filtered through a 0.22-μm syringe filter for chemical analysis. For As-amended batches, 150 μL of filtrate was used for measurement of As (III) with a $KMnO_4$-reactive spectrophotometric method [34]. Residual filtrate was stored at -20 ^{o}C for the measurement of N species (nitrate and ammonium) with a Lachat QuickChem8000 Flow Injection Analyzer (Lachat Instrument, Milwaukee, WI) and As speciation and accurate quantification by Inductively Coupled Plasma - Mass Spectrometry (ICP-MS) in the Environmental Analysis Laboratory at Southern Cross University (SCU). For $^{13}CO_2$ quantification a 0.5 mL aqueous sample was immediately injected into a 3 mL helium flushed (for 5 mins) Exetainer vials (Labco) and preserved at -20 ^{o}C. Prior to measurement, 0.2 mL 1M HCl was injected into each thawed sample to extract CO_2 which was analysed using gas chromatography-mass spectrometry (7890A/5975C; Agilent) and the $^{13}CO_2$ ratio calculated as described in Scheller *et al.*

DNA and RNA extraction

Nucleic acids were extract from 2 mL cell suspension samples from each batch at 24 and 36 hrs. Half of the cell suspension was processed using a FastRNA Pro Soil-Direct Kit (MP Biomedicals, USA) for RNA extraction following the manufacturer's protocol. RNA concentrations were quantified using the NanoDrop Spectrophotometer (Thermo Scientific). RNAseOUT (Invitrogen) was added to the extracted RNA sample to a concentration of 5% [v/v] before preservation at -80 ^{o}C. The remaining biomass (1 mL) was used for DNA extraction using a FastDNA SPIN kit for soil (MP Biomedicals, USA) following the manufacturer's protocol. DNA concentrations were quantified using the Qubit HS dsDNA assay kit (Invitrogen).

DNA and RNA library preparation and sequencing

Paired-end libraries were prepared for all DNA extracts using the Illumina DNA Prep Kit (Illumina). The libraries were quantified using the Qubit dsDNA HS assay kit (Invitrogen) and sequenced using the Illumina NovaSeq to produce 2 Gb of shotgun metagenomic paired-end reads (2 × 150 bp). Metatranscriptomes were prepared from RNA extracted from the 36 hr timepoints of all batches.

RNA extracts were cleaned of residual DNA twice using the RNA Clean & Concentrator-5 kit (Zymo Research), including DNase I treatments. Following clean-up, RNA extracts were quantified using the Qubit HS RNA assay kit and RNA integrity was assessed using the TapeStation (Agilent). Ribosomal-RNA depletion, cDNA generation and library preparation were done using the Illumina Ribozero Plus Kit following manufacturers protocol by the Australian Centre for Ecogenomics (ACE). RNA libraries were sequenced on a Novoseq6000 at ACE, generating ~9 Gb per 30 million paired-end reads (2 × 150 bp) per sample.

Metagenomic analysis

Quality control, binning, and assembly of metagenomes

Quality of the returned reads was assessed using FastQC v0.11.9 (https://github.com/s-andrews/FastQC) and MultiQC v1.11, and reads were then trimmed using Cutadapt v3.5 [35]. Metagenomes were assembled using MetaSPAdes v3.11.1. MAGS were binned for each sample using Aviary v0.2.0 (https://github.com/rhysnewell/aviary). MAG quality was determined using CheckM2 v0.0.1 [36], and dereplicated at 95% average nucleotide identity (ANI) using CoverM v0.6.1 via the cluster function (https://github.com/wwood/CoverM). MAGs with ≥70% completeness and ≤10% contamination were retained. These MAGs were dereplicated with previously recovered closed MAGs obtained in a previous study from the same seed bioreactor using a combination of short and long-read sequencing [37]. Microbial community profiles of each bioreactor batch were prepared by mapping paired-end reads to the retained MAGs using the CoverM v0.6.1 genome function. MAGs were assigned taxonomy using GTDB-Tk v2.1.0 [38] which assigns GTDB release 07-RS207 taxonomy [39].

Functional annotation

ORFs were called for all MAGs using Prokka v1.14.6 [40]. ORFs were functionally annotated with KEGG Orthology (KO)[41] and PFAMs[42] using EnrichM v0.6.3 (https://github.com/geronimp/enrichM) via the annotate function. Additional functional annotation was done using METABOLIC-G [43]. Putative multiheme type *c* cytochromes (MHCs) were identified by searching for ORFs possessing >3 CXXCH motifs, and further checking for cytochrome *c* domains via NCBI CD-Batch search [44,45].

The presence of oxidoreductases that might mediate arsenate reduction in the reactor batches was investigated for all MAGs. Putative oxidoreductases were identified by screening for the molybdopterin oxidoreductase domain denoted by PFAM ID PF00384 [42]. The function of the molybdopterin oxidoreductase ORFs was inferred phylogenetically alongside a set of curated molybdopterin oxidoreductases retrieved from a previous publication [6]. First, the ORFs were aligned using Muscle v5 [30] with default parameters. Then, a protein tree of the alignment was constructed using IQ-Tree [31] with bootstrapping of 1000 replicates and the LG+F+R9 model. The protein tree was visualised on iTOL [32].

315 **Metatranscriptomic analysis**

316 ***Read mapping of mRNA and differential gene expression analysis***

317 The metatranscriptomic paired-end reads were processed using the pipeline embedded in
318 TranscriptM v.0.5 (https://github.com/sternp/transcriptm). To summarise, TranscriptM first assessed
319 quality of reads using Kneaddata (https://github.com/biobakery/kneaddata), and then trimmed reads
320 using Trimmomatic [46]. BAM files were generated by mapping trimmed reads to MAGs using CoverM
321 v0.6.1 Make and filtered via CoverM v0.6.1 Filter. DNA contamination was assessed based on the
322 directionality of transcripts and removed from BAM files using the Bioconductor R package,
323 StrandCheckR v1.15.0. Finally, raw count tables were generated using the Subread v2.0.3 package
324 (http://subread.sourceforge.net/), and TPM values were calculated using the following equation:

325 $$\mathrm{TPM} = \frac{\mathrm{rg} \times \mathrm{rl} \times 10^6}{\mathrm{flg} \times \mathrm{T}}$$

326 Where rg = reads mapped to gene g, rl = read length, flg = feature length (or CDS length), and
327 T = sum of rg*rl/flg for all genes. Differential gene expression analysis was performed for *Ca*. 'M.
328 nitroreducens' using the Bioconductor R package, DESeq2 v3.15 [47], using the raw count table supplied
329 by TranscriptM.

330 ## Author contributions

331 SJM, XZ, AOL, GWT, and SH conceived the study. GHJ, XZ, SH, and SJM planned the experiments.
332 GHJ performed the DNA and RNA extraction and preparation for metagenomics and
333 metatranscriptomics sequencing. XZ conducted the batch incubations and corresponding chemical
334 analyses. GHJ and AOL performed and interpreted bioinformatics analyses. GHJ, XZ, SH and SJM,
335 wrote the manuscript in consultation with all authors.

336 ## Competing interests

337 The authors declare no competing interests.

338

339

Intext Figures & Tables

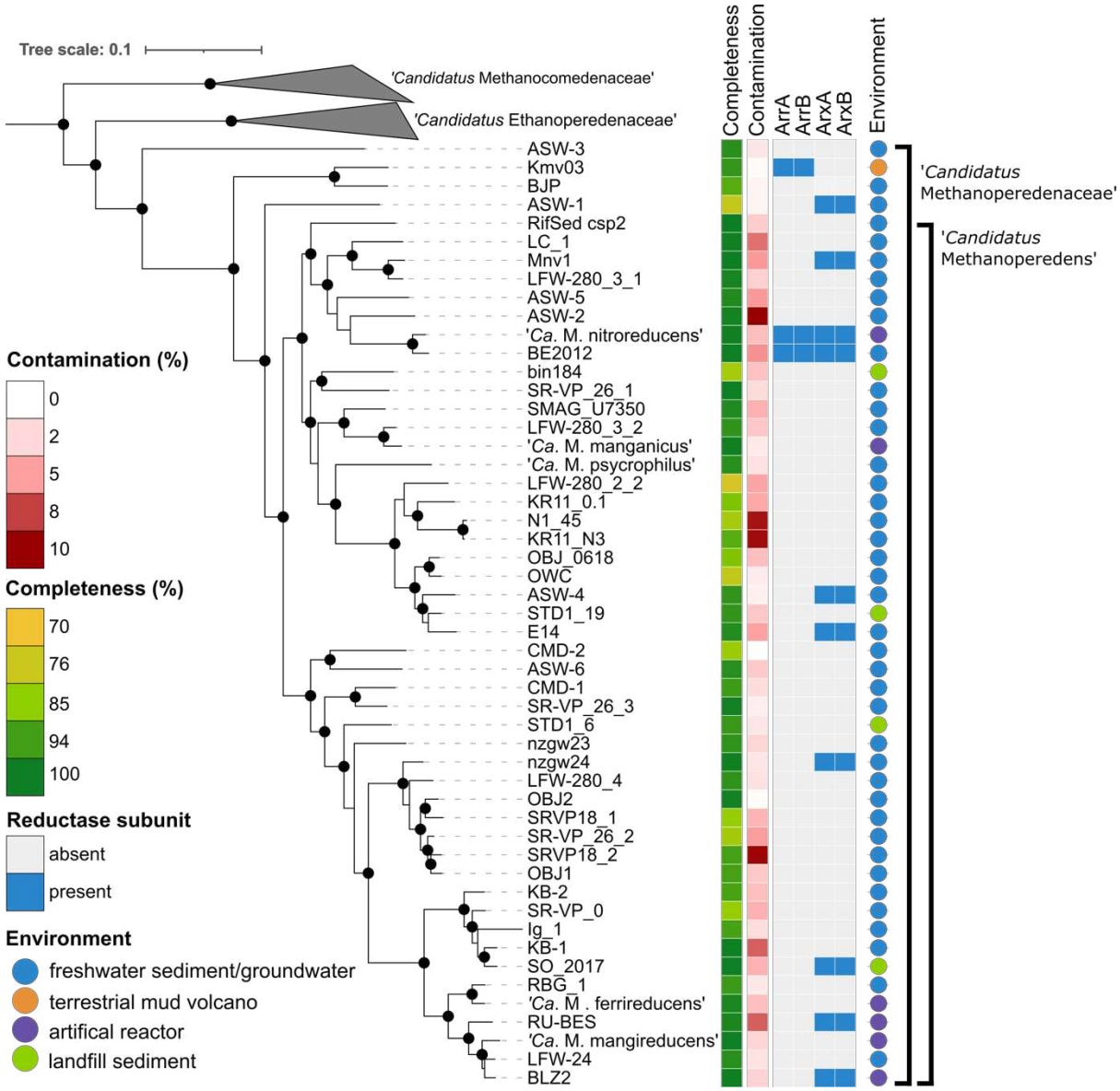


Figure 1: Phylogenetic placement of '*Ca*. Methanoperedenaceae' metagenome assembled genomes (MAGs) and distribution of Arr and Arx catalytic subunits across lineage. MAGs were retrieved from the Genome Taxonomy Database (GTDB) release 226. MAG completeness and contamination were predicted by CheckM2 (see methods), and environment indicates the isolation source of the MAG according to associated publications or NCBI BioProject metadata. The genome tree was inferred using maximum-likelihood with a concatenated set of 122 archaeal specific marker genes. Black circles represent bootstrap support > 85% with 1000 replicates.

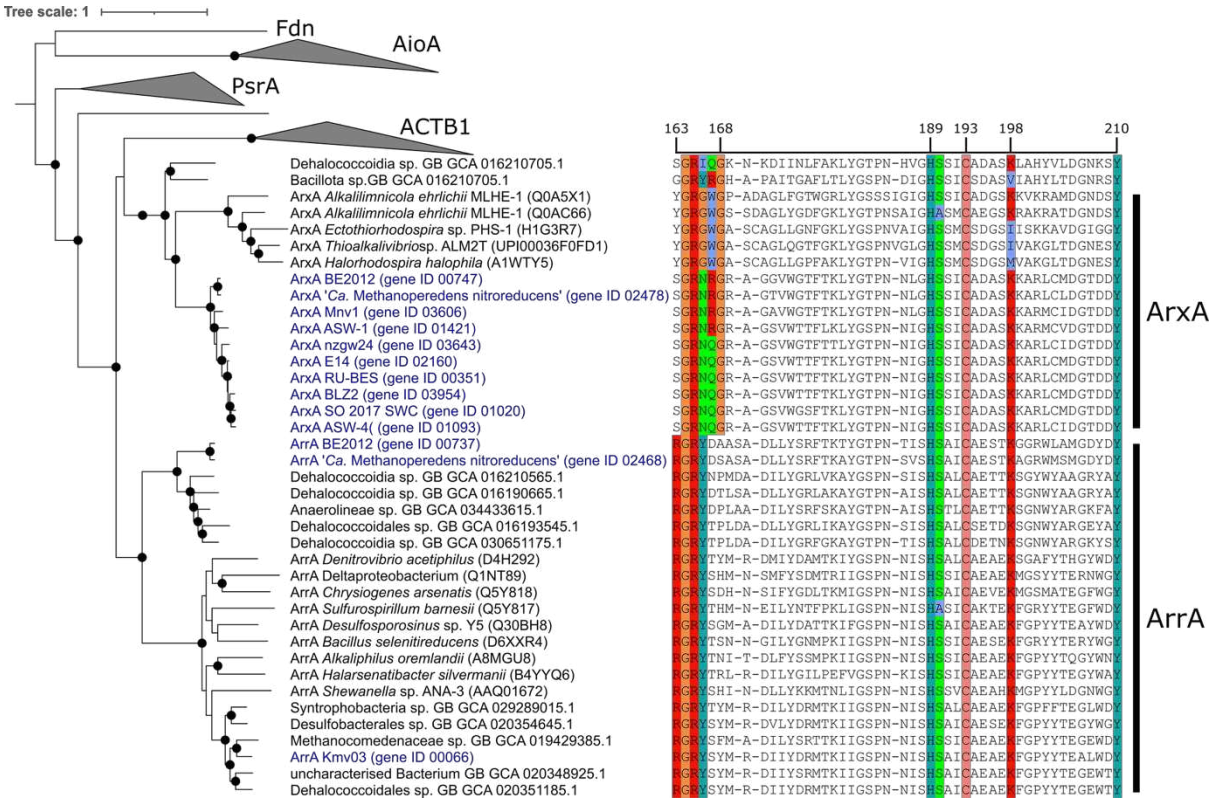


Figure 2: Phylogenetic inference of arsenate reductase (Arr) and arsenite oxidase (Arx) subunit A and multiple sequence alignment of predicted active side residues. Representative ArrA/ArxA proteins are included, as well as blastp hits (see methods, **S2, S6**) derived from MAGs deposited in the Genome Taxonomy Database, with Genbank accessions indicated in brackets. Members of '*Ca*. Methanoperedenaceae' are labelled blue. The active side residues are indicated by colour according to the ClustalW colour scheme and were predicted based on a previous study, with the residue position annotated to be consistent with *Shewanella* ANA-3 ArrA (Glasser et al., 2018). ArrA enzymes contain an RGRY motif (residues 163-166); bacterial ArxA sequences contain a GRGWG motif (residues 164-168), meanwhile '*Ca*. Methanoperedenaceae'-Arx contain a GRN(R/Q)G motif in the same position. Other active-site residues identified in Glasser et al. (2018) are generally conserved across all enzymes (residues 189, 193, 198, 210). Black dots indicate bootstrap support > 85% (1000 replicates).

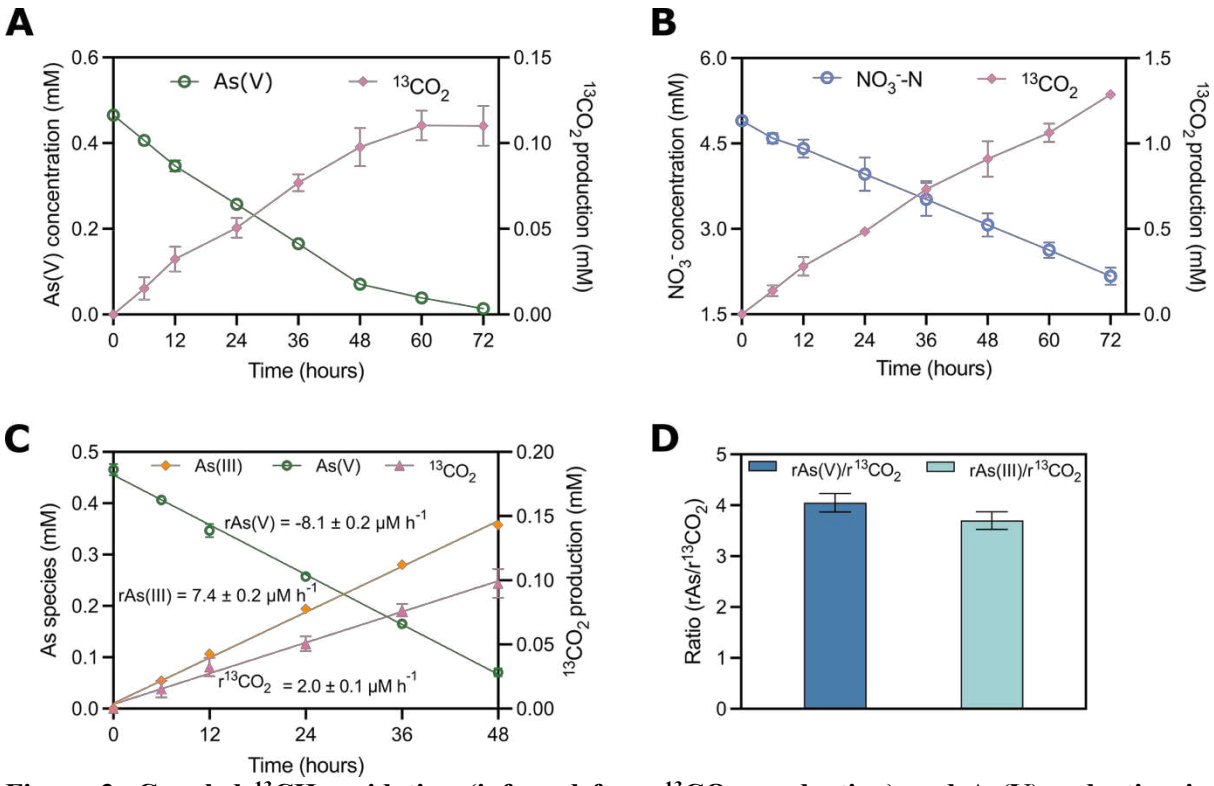


Figure 3: Coupled $^{13}CH_4$ oxidation (inferred from $^{13}CO_2$ production) and As(V) reduction in batch incubations by '*Ca.* M. nitroreducens' enrichment culture. Error bars indicate standard deviations of two independent biological replicates. **(A)** Monitoring of As(V), and $^{13}CO_2$ accumulation during the operation of the arsenate-fed batch. (**B)** Monitoring of NO_3^- concentration and $^{13}CO_2$ accumulation during nitrate-fed batch operation. Labelled ^{13}C was supplied at time 0 as $^{13}CH_4$. **(C)** Profiles and rates of As(V) reduction, As(III) production and $^{13}CO_2$ production during incubation with As(V) and $^{13}CH_4$. Rates are determined by linear regression from the respective measured concentrations (during the period of 0 to 48 h). The confidence level for fitting curves was 95%. **(D)** Ratios of As(V) reduction and As(III) production rates, respectively, to the AOM rate ($^{13}CO_2$ production rate) in the incubation with As(V) and $^{13}CH_4$.

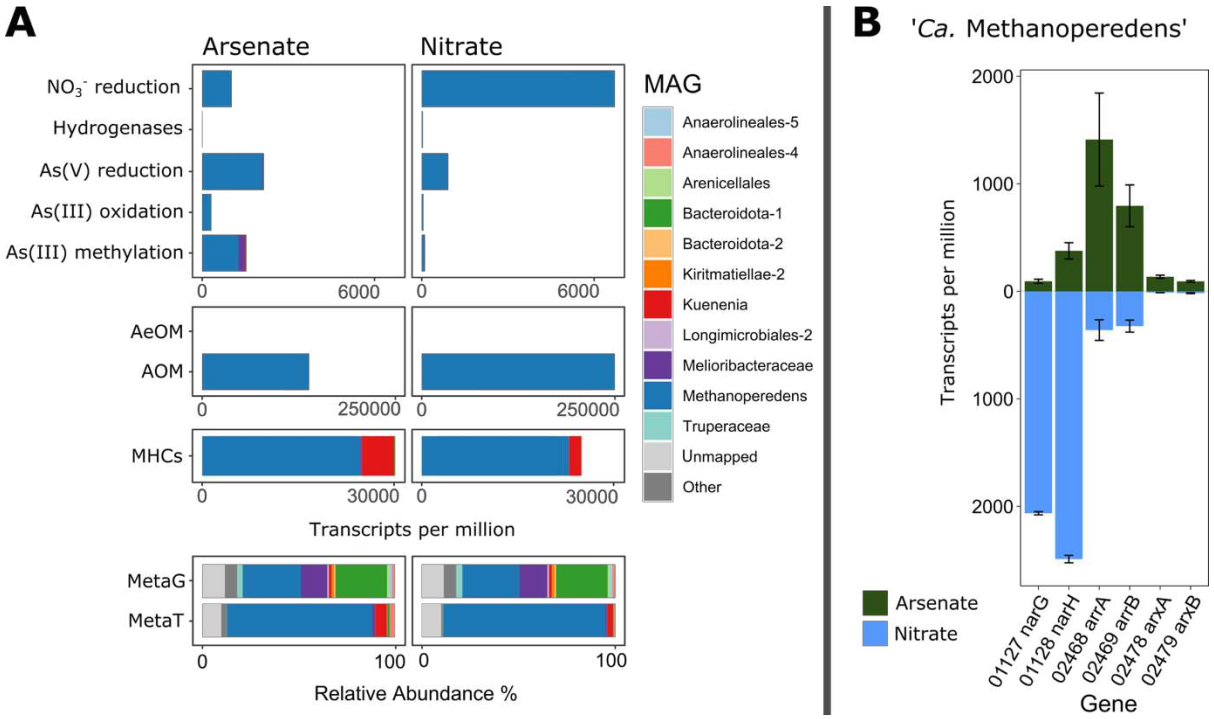


Figure 4: Microbial community composition and transcriptional activity under arsenate-reducing *versus* nitrate-reducing conditions. Transcripts per million (TPM) and relative abundances are shown as the average of two biological replicates. **A)** Metagenomic (MetaG) and metatranscriptomic (MetaT) profile of the microbial community abundant organisms and key pathways from arsenate-fed *versus* nitrate-fed anaerobic methane oxidising batch incubations at 36 hours. 'AeOM' = Aerobic methane oxidation; AOM = Anaerobic oxidation of methane; 'MHCs' = multiheme type *c* cytochromes. **B)** Differential expression of key terminal oxidoreductase complexes by '*Ca*. Methanoperedens nitroreducens' under arsenate-fed *versus* nitrate-fed anaerobic methane oxidising batch incubations at 36 hours. Error bars indicate standard deviation.

References

1 Cai, C. *et al.* A methanotrophic archaeon couples anaerobic oxidation of methane to Fe(III) reduction. *The ISME Journal* **12**, 1929-1939 (2018). https://doi.org/10.1038/s41396-018-0109-x

2 Leu, A. O. *et al.* Anaerobic methane oxidation coupled to manganese reduction by members of the Methanoperedenaceae. *The ISME Journal* **14**, 1030-1041 (2020). https://doi.org/10.1038/s41396-020-0590-x

3 Haroon, M. F. *et al.* Anaerobic oxidation of methane coupled to nitrate reduction in a novel archaeal lineage. *Nature* **500**, 567-570 (2013). https://doi.org/10.1038/nature12375

4 Ettwig, K. F. *et al.* Archaea catalyze iron-dependent anaerobic oxidation of methane. *Proc Natl Acad Sci U S A* **113**, 12792-12796 (2016). https://doi.org/10.1073/pnas.1609534113

5 Raghoebarsing, A. A. *et al.* A microbial consortium couples anaerobic methane oxidation to denitrification. *Nature* **440**, 918-921 (2006). https://doi.org/10.1038/nature04617

6 Leu, A. O. *et al.* Lateral Gene Transfer Drives Metabolic Flexibility in the Anaerobic Methane-Oxidizing Archaeal Family Methanoperedenaceae. *mBio* **11**, 10.1128/mbio.01325-01320 (2020). https://doi.org/doi:10.1128/mbio.01325-20

7 Glodowska, M. *et al.* Arsenic mobilization by anaerobic iron-dependent methane oxidation. *Communications Earth & Environment* **1**, 42 (2020). https://doi.org/10.1038/s43247-020-00037-y

8 Glodowska, M. *et al.* Fermentation, methanotrophy and methanogenesis influence sedimentary Fe and As dynamics in As-affected aquifers in Vietnam. *Science of The Total Environment* **779**, 146501 (2021). https://doi.org/https://doi.org/10.1016/j.scitotenv.2021.146501

9 Shi, L. D. *et al.* Coupled anaerobic methane oxidation and reductive arsenic mobilization in wetland soils. *Nature Geoscience* **13**, 799-+ (2020). https://doi.org/10.1038/s41561-020-00659-z

10 Jiang, O.-Y. *et al.* Arsenic Reduces Methane Emissions from Paddy Soils: Insights from Continental Investigation and Laboratory Incubations. *Environmental Science & Technology* **58**, 17685-17694 (2024). https://doi.org/10.1021/acs.est.4c06809

11 Zhou, Y. *et al.* Anaerobic methane oxidation coupled to arsenate reduction in paddy soils: Insights from laboratory and field studies. *Chemosphere*, 137055 (2022). https://doi.org/https://doi.org/10.1016/j.chemosphere.2022.137055

12 Ospino, M. C., Kojima, H. & Fukui, M. Arsenite Oxidation by a Newly Isolated Betaproteobacterium Possessing arx Genes and Diversity of the arx Gene Cluster in Bacterial Genomes. *Front. Microbiol.* **10** (2019). https://doi.org/10.3389/fmicb.2019.01210

13 Szyttenholm, J. *et al.* The controversy on the ancestral arsenite oxidizing enzyme; deducing evolutionary histories with phylogeny and thermodynamics. *Biochimica et Biophysica Acta (BBA) - Bioenergetics* **1861**, 148252 (2020). https://doi.org/https://doi.org/10.1016/j.bbabio.2020.148252

14 Glasser, N. R., Oyala, P. H., Osborne, T. H., Santini, J. M. & Newman, D. K. Structural and mechanistic analysis of the arsenate respiratory reductase provides insight into environmental arsenic transformations. *Proceedings of the National Academy of Sciences* **115**, E8614-E8623 (2018). https://doi.org/10.1073/pnas.1807984115

15 Zhao, X.-D., Gao, Z.-Y., Peng, J., Konstantinidis, K. T. & Zhang, S.-Y. Various microbial taxa couple arsenic transformation to nitrogen and carbon cycling in paddy soils. *Microbiome* **12**, 238 (2024). https://doi.org/10.1186/s40168-024-01952-4

16 Becraft, E. D. *et al.* Evolutionary stasis of a deep subsurface microbial lineage. *The ISME Journal* **15**, 2830-2842 (2021). https://doi.org/10.1038/s41396-021-00965-3

17 Mardanov, A. V., Kadnikov, V. V., Beletsky, A. V. & Ravin, N. V. Sulfur and Methane-Oxidizing Microbial Community in a Terrestrial Mud Volcano Revealed by Metagenomics. *Microorganisms* **8**, 1333 (2020).

18 Ouboter, H. T. *et al.* Methane-Dependent Extracellular Electron Transfer at the Bioanode by the Anaerobic Archaeal Methanotroph "Candidatus Methanoperedens". *Front Microbiol* **13**, 820989 (2022). https://doi.org/10.3389/fmicb.2022.820989

19 Timmers, P. H. *et al.* Reverse Methanogenesis and Respiration in Methanotrophic Archaea. *Archaea* **2017**, 1654237 (2017). https://doi.org/10.1155/2017/1654237
20 Palmer, T. & Berks, B. C. The twin-arginine translocation (Tat) protein export pathway. *Nature Reviews Microbiology* **10**, 483-496 (2012). https://doi.org/10.1038/nrmicro2814
21 Omelchenko, M. V., Makarova, K. S., Wolf, Y. I., Rogozin, I. B. & Koonin, E. V. Evolution of mosaic operons by horizontal gene transfer and gene displacement in situ. *Genome Biology* **4**, R55 (2003). https://doi.org/10.1186/gb-2003-4-9-r55
22 Zhang, X. *et al.* Multi-heme cytochrome-mediated extracellular electron transfer by the anaerobic methanotroph 'Candidatus Methanoperedens nitroreducens'. *Nature Communications* **14**, 6118 (2023). https://doi.org/10.1038/s41467-023-41847-w
23 Arshad, A. *et al.* A Metagenomics-Based Metabolic Model of Nitrate-Dependent Anaerobic Oxidation of Methane by Methanoperedens-Like Archaea. *Front Microbiol* **6**, 1423 (2015). https://doi.org/10.3389/fmicb.2015.01423
24 Malasarn, D., Keeffe, J. R. & Newman, D. K. Characterization of the Arsenate Respiratory Reductase from *Shewanella* sp. Strain ANA-3. *J Bacteriol* **190**, 135 (2008). https://doi.org/10.1128/JB.01110-07
25 Krafft, T. & Macy, J. M. Purification and characterization of the respiratory arsenate reductase of Chrysiogenes arsenatis. *European Journal of Biochemistry* **255**, 647-653 (1998). https://doi.org/https://doi.org/10.1046/j.1432-1327.1998.2550647.x
26 Badilla, C. *et al.* A new family of periplasmic-binding proteins that sense arsenic oxyanions. *Scientific Reports* **8**, 6282 (2018). https://doi.org/10.1038/s41598-018-24591-w
27 Zargar, K. *et al.* ArxA, a new clade of arsenite oxidase within the DMSO reductase family of molybdenum oxidoreductases. *Environ Microbiol* **14**, 1635-1645 (2012). https://doi.org/10.1111/j.1462-2920.2012.02722.x
28 Oremland, R. S. & Stolz, J. F. Arsenic, microbes and contaminated aquifers. *Trends Microbiol* **13**, 45-49 (2005). https://doi.org/10.1016/j.tim.2004.12.002
29 Podgorski, J. & Berg, M. Global threat of arsenic in groundwater. *Science* **368**, 845-850 (2020). https://doi.org/10.1126/science.aba1510
30 Edgar, R. C. MUSCLE v5 enables improved estimates of phylogenetic tree confidence by ensemble bootstrapping. *bioRxiv*, 2021.2006.2020.449169 (2021). https://doi.org/10.1101/2021.06.20.449169
31 Nguyen, L.-T., Schmidt, H. A., von Haeseler, A. & Minh, B. Q. IQ-TREE: a fast and effective stochastic algorithm for estimating maximum-likelihood phylogenies. *Mol Biol Evol* **32**, 268-274 (2015). https://doi.org/10.1093/molbev/msu300
32 Letunic, I. & Bork, P. Interactive Tree Of Life (iTOL) v5: an online tool for phylogenetic tree display and annotation. *Nucleic Acids Research* **49**, W293-W296 (2021). https://doi.org/10.1093/nar/gkab301
33 Rascovan, N., Maldonado, J., Vazquez, M. P. & Eugenia Farías, M. Metagenomic study of red biofilms from Diamante Lake reveals ancient arsenic bioenergetics in haloarchaea. *The ISME Journal* **10**, 299-309 (2016). https://doi.org/10.1038/ismej.2015.109
34 Bahar, M. M., Mahbub, K. R., Naidu, R. & Megharaj, M. A simple spectrophotometric method for rapid quantitative screening of arsenic bio-transforming bacteria. *Environmental Technology & Innovation* **19**, 100840 (2020). https://doi.org/https://doi.org/10.1016/j.eti.2020.100840
35 Martin, M. Cutadapt removes adapter sequences from high-throughput sequencing reads. *2011* **17**, 3 %J EMBnet.journal (2011). https://doi.org/10.14806/ej.17.1.200
36 Chklovski, A., Parks, D. H., Woodcroft, B. J. & Tyson, G. W. CheckM2: a rapid, scalable and accurate tool for assessing microbial genome quality using machine learning. *bioRxiv*, 2022.2007.2011.499243 (2022). https://doi.org/10.1101/2022.07.11.499243
37 McIlroy, S. J. *et al.* Anaerobic methanotroph 'Candidatus Methanoperedens nitroreducens' has a pleomorphic life cycle. *Nat Microbiol* **8**, 321-331 (2023). https://doi.org/10.1038/s41564-022-01292-9
38 Chaumeil, P.-A., Mussig, A. J., Hugenholtz, P. & Parks, D. H. GTDB-Tk: a toolkit to classify genomes with the Genome Taxonomy Database. *Bioinformatics* **36**, 1925-1927 (2020). https://doi.org/10.1093/bioinformatics/btz848

39 Parks, D. H. *et al.* GTDB: an ongoing census of bacterial and archaeal diversity through a phylogenetically consistent, rank normalized and complete genome-based taxonomy. *Nucleic Acids Research* **50**, D785-D794 (2022). https://doi.org/10.1093/nar/gkab776

40 Seemann, T. Prokka: rapid prokaryotic genome annotation. *Bioinformatics* **30**, 2068-2069 (2014). https://doi.org/10.1093/bioinformatics/btu153

41 Kanehisa, M., Furumichi, M., Tanabe, M., Sato, Y. & Morishima, K. KEGG: new perspectives on genomes, pathways, diseases and drugs. *Nucleic Acids Res* **45**, D353-d361 (2017). https://doi.org/10.1093/nar/gkw1092

42 Mistry, J. *et al.* Pfam: The protein families database in 2021. *Nucleic Acids Research* **49**, D412-D419 (2021). https://doi.org/10.1093/nar/gkaa913

43 Zhou, Z. *et al.* METABOLIC: high-throughput profiling of microbial genomes for functional traits, metabolism, biogeochemistry, and community-scale functional networks. *Microbiome* **10**, 33 (2022). https://doi.org/10.1186/s40168-021-01213-8

44 Wang, J. *et al.* The conserved domain database in 2023. *Nucleic Acids Research* **51**, D384-D388 (2022). https://doi.org/10.1093/nar/gkac1096

45 Marchler-Bauer, A. *et al.* CDD/SPARCLE: functional classification of proteins via subfamily domain architectures. *Nucleic Acids Res* **45**, D200-d203 (2017). https://doi.org/10.1093/nar/gkw1129

46 Bolger, A. M., Lohse, M. & Usadel, B. Trimmomatic: a flexible trimmer for Illumina sequence data. *Bioinformatics* **30**, 2114-2120 (2014). https://doi.org/10.1093/bioinformatics/btu170

47 Love, M. I., Huber, W. & Anders, S. Moderated estimation of fold change and dispersion for RNA-seq data with DESeq2. *Genome Biol* **15**, 550 (2014). https://doi.org/10.1186/s13059-014-0550-8

Supplementary Files

This is a list of supplementary files associated with this preprint. Click to download.

- Joycesuppfigs.pdf
- Joycesupplementarydatasets.xlsx